



© 2022 Geological Society of America. For permission to copy, contact editing@geosociety.org.

Manuscript received 20 December 2021 Revised manuscript received 22 February 2022 Manuscript accepted 27 February 2022

Published online 9 May 2022

# Multiple phyla, one time resolution? Similar time averaging in benthic foraminifera, mollusk, echinoid, crustacean, and otolith fossil assemblages

Rafał Nawrot<sup>1</sup>, Michaela Berensmeier<sup>1</sup>, Ivo Gallmetzer<sup>1</sup>, Alexandra Haselmair<sup>1</sup>, Adam Tomašových<sup>2</sup> and Martin Zuschin<sup>1</sup>
<sup>1</sup>Department of Palaeontology, University of Vienna, 1090 Vienna, Austria
<sup>2</sup>Earth Science Institute, Slovak Academy of Sciences, 84005 Bratislava, Slovakia

#### ABSTRACT

Time averaging of fossil assemblages determines temporal precision of paleoecological and geochronological inferences. Taxonomic differences in intrinsic skeletal durability are expected to produce temporal mismatch between co-occurring species, but the importance of this effect is difficult to assess due to lack of direct estimates of time averaging for many higher taxa. Moreover, burial below the taphonomic active zone and early diagenetic processes may alleviate taxonomic differences in disintegration rates in subsurface sediments. We compared time averaging across five phyla of major carbonate producers co-occurring in a sediment core from the northern Adriatic Sea shelf. We dated individual bivalve shells, foraminiferal tests, tests and isolated plates of irregular and regular echinoids, crab claws, and fish otoliths. In spite of different skeletal architecture, mineralogy, and life habit, all taxa showed very similar time averaging varying from ~1800 to ~3600 yr (interquartile age ranges). Thus, remains of echinoids and crustaceans—two groups with multi-elemental skeletons assumed to have low preservation potential—can still undergo extensive age mixing comparable to that of the co-occurring mollusk shells. The median ages of taxa differed by as much as ~3700 yr, reflecting species-specific timing of seafloor colonization during the Holocene transgression. Our results are congruent with sequestration models invoking taphonomic processes that minimize durability differences among taxa. These processes together with temporal variability in skeletal production can overrule the effects of durability in determining temporal resolution of multi-taxic fossil assemblages.

## INTRODUCTION

Time averaging—mixing of remains of organisms that lived at different times in a single sedimentary layer—dictates the temporal resolution of the fossil record (Kowalewski and Bambach, 2008; Kidwell, 2013). Stratigraphic co-occurrence of organisms separated by centuries or millennia affects not only paleoecological inferences but also the resolution of geochemical and geochronological records based on their biomineralized remains. The extent of time averaging is expected to correlate with intrinsic skeletal durability (e.g., Kowalewski, 1997): remains of taxa with robust skeletons should survive longer in the taphonomic active zone (TAZ) and thus be, on average, older and more time averaged than co-occurring remains of fragile taxa (Broecker and Clark, 2011; Mekik, 2014), as observed in molluscan and foraminiferal assemblages

(e.g., Barker et al., 2007; Kosnik et al., 2009). The variation in durability across higher taxa may be even the main factor controlling the temporal resolution of fossil assemblages, as suggested by the millennial time averaging of robust bivalve shells contrasting with the yearly resolution of more fragile echinoid tests (Kowalewski et al., 2018).

The evaluation of this hypothesis, however, is hindered by narrow taxonomic coverage of the previous dating efforts, which, with a few exceptions (e.g., Krause et al., 2010; Kowalewski et al., 2018; Lin et al., 2019; Albano et al., 2020), focused mostly on aragonitic bivalves (Kidwell, 2013). Moreover, the effects of durability on time averaging can be overwhelmed by variation in timing of skeletal production (Tomašových et al., 2019a, 2019b) and by spatial variation in sedimentation rates and depth of mixing (Krause et al.,

2010; Albano et al., 2020). Finally, differences in time averaging documented in the TAZ do not necessarily translate into the subsurface stratigraphic record (Olszewski, 2004). Sequestration processes that lead to burial and early diagenetic stabilization allow fragile skeletal elements to escape rapid disintegration near the sediment-water interface (Olszewski, 2004; Tomašových et al., 2014) and may generate highly time-averaged assemblages formed by fragile remains.

We used individually dated specimens sampled from the subsurface stratigraphic record of the northern Adriatic Sea shelf to quantify variation in time averaging among five major phyla: Foraminifera (foraminiferal tests), Mollusca (bivalve shells), Echinodermata (echinoid tests and plates), Arthropoda (crab claws), and Chordata (fish otoliths), which play an important role in marine ecosystems. To contrast the effects of taxonomic variation in durability with the role of sequestration and sedimentation rates, we compared the observed extent of time averaging to (1) the ranking of species according to their mineralogical stability and size, and (2) the scale of time averaging expected from the long-term sedimentation rate and the bioturbation depth.

# MATERIAL AND METHODS Study Area and Sampling

The Gulf of Trieste (Fig. 1) is located in the northeastern Adriatic Sea. Its offshore parts, with a maximum depth of 25 m, have limited terrigenous input, low net sedimentation rates (<0.5 mm/yr), and reduced thickness of marine Holocene deposits (<5 m) compared to more onshore locations (Trobec et al., 2018). The sites currently at  $\sim\!20$  m water depth were flooded at ca. 9500–10,000 yr B.P. during the Holocene marine transgression (Fig. 1).

CITATION: Nawrot, R., et al., 2022, Multiple phyla, one time resolution? Similar time averaging in benthic foraminifera, mollusk, echinoid, crustacean, and otolith fossil assemblages: Geology, v. 50, p. 902–906, https://doi.org/10.1130/G49970.1

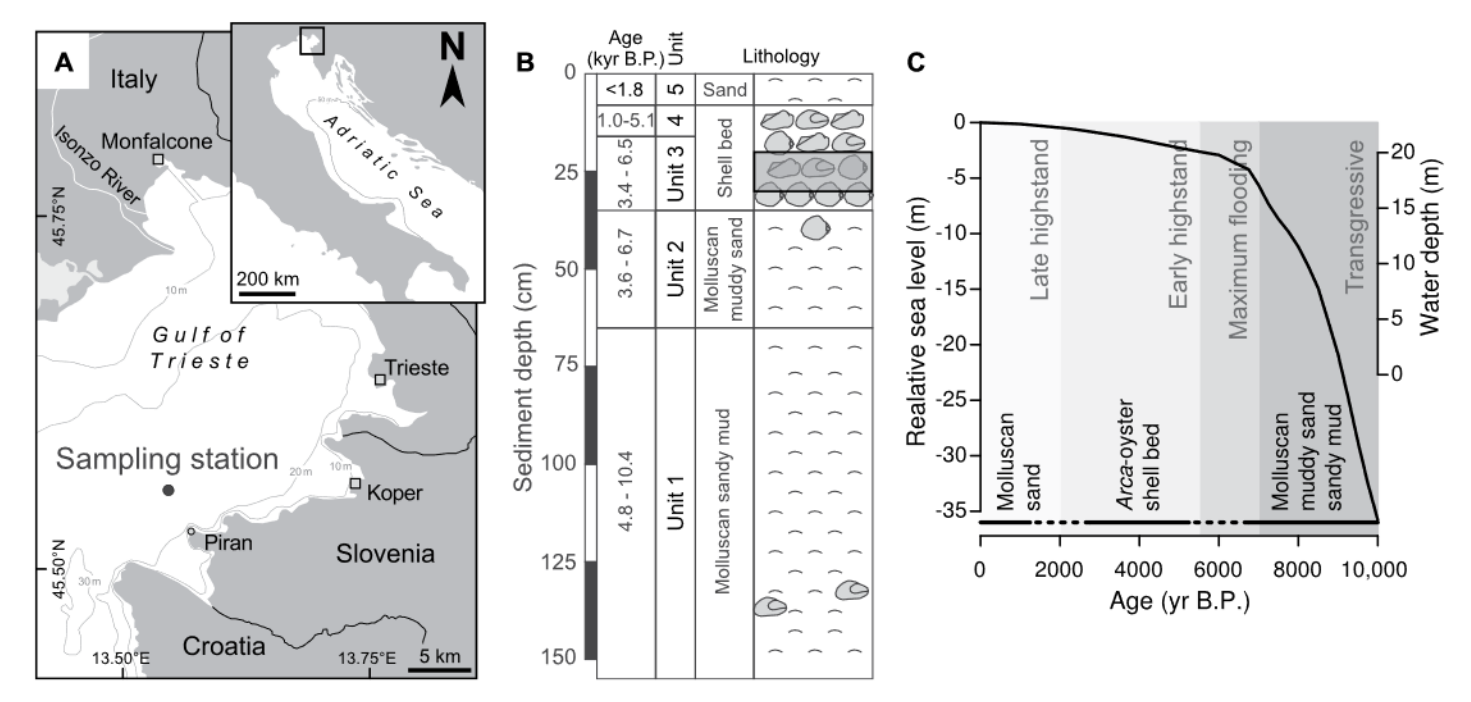


Figure 1. (A) Location of sampling station in the Gulf of Trieste, Adriatic Sea. Bathymetric contours are in m, contour interval is 10 m. (B) Stratigraphy of core Piran 2 M53 with position of the sampled interval (gray rectangle) (modified from Tomašových et al., 2019a). Age of the stratigraphic units is based on the 25<sup>th</sup> and 75<sup>th</sup> percentiles of bivalve shell ages. (C) Relative sea level in the Gulf of Trieste over the past 10 k.y. (Lambeck et al., 2011) and corresponding water depth at the coring station currently located at 22.7 m below sea level, with major sea-level phases in northern Adriatic Sea (Gallmetzer et al., 2019). Age ranges of the stratigraphic units (Mautner et al., 2018) are marked with horizontal lines with dashed intervals indicating uncertainty around their boundaries.

In 2013 CE, three 150-cm-long piston cores were collected 4 km off Piran (Slovenia; 45.563200°N, 13.537033°E) in the southern Gulf of Trieste at a depth of 22.7 m (Fig. 1A; Mautner et al., 2018). The cores were subdivided into five stratigraphic units, which correspond chronologically to the major sea-level phases in the northern Adriatic (Figs. 1B and 1C; Gallmetzer et al., 2019). One 16-cm-diameter core was sliced into 2- to 5-cm-thick increments and wet sieved. Mollusk shells, foraminiferal tests, elements of echinoderms and crustaceans, and fish otoliths were picked from the 1 mm sieve fraction. The core age model, stratigraphic framework, and changes in mollusk assemblages were reported by Mautner et al. (2018), Gallmetzer et al. (2019), and Tomašových et al. (2019a). Surface sediments at this coring station consist of skeletal muddy sands, underlain by a densely packed, poorly sorted molluscan shell bed located at 8-35 cm below the sediment surface (Fig. 1B). The base of the shell bed, interpreted as the maximum flooding zone, was dated to ca. 6500 yr B.P. (Tomašových et al., 2019a). The material analyzed here comes from two increments at 20-25 cm and 25-30 cm depth that were combined to obtain adequate sample sizes.

# Target Taxa

Species were selected based on their abundance and to cover a wide range of skeletal properties and life habits (Table S1 in the Sup-

plemental Material1). The aragonitic shells of bivalves Corbula gibba and Gouldia minima were previously dated using 14C-calibrated amino acid racemization (AAR) methods (Tomašových et al., 2019a). Here, we present the radiocarbon ages of two benthic foraminifera (the high-Mg calcitic milliolid Adelosina intricata and the low-Mg calcitic rotaliid Elphidium crispum), the minute irregular clypeasteroid echinoid Echinocyamus pusillus, the regular camarodont echinoids Paracentrotus lividus and Psammechinus microtuberculatus (all echinoids with high-Mg calcitic stereom), the brachyuran crustacean Pilumnus sp. (with low-Mg calcitic chelae), and the teleost fish Gobius niger (with aragonitic otoliths). We selected only complete bivalve valves or fragments with umbo, foraminifera with >60% of the test preserved, complete or partly preserved (>40%) tests of E. pusillus, isolated madreporite plates of the two regular echinoid species (which were analyzed together to increase sample size), isolated elements of chelae (dactyli and propodi) of Pilumnus sp., and sagittal otoliths of G. niger. All unique specimens were dated, except foraminifera and bivalves, for which 20–30 specimens were randomly selected per sample.

#### Radiocarbon Dating

Six taxa not dated by AAR were analyzed with the direct carbonate accelerator mass spectrometry radiocarbon technique (Bush et al., 2013). Application of powdered carbonate targets allows dating of submilligram samples and produces ages that are consistent with the results of the standard graphite <sup>14</sup>C method (Bright et al., 2021). Radiocarbon ages were calibrated to calendar ages (see the Supplemental Material) and are reported in years before present (yr B.P., i.e., relative to the year 1950 CE).

### **Data Analysis**

We used the interquartile age range (IOR) to quantify the extent of time averaging of each taxon. Although IQR is less sensitive to sample size than other measures of dispersion, these values should be treated as minimum estimates due to relatively small sample sizes (Table 1; Olszewski, 1999). Higher age errors associated with AAR dating of bivalve shells can inflate estimates of time averaging, but accounting for this effect does not affect our conclusions (Fig. S1 in the Supplemental Material). We estimated biascorrected percentile confidence intervals around the IQRs and median ages using a bootstrap procedure with 10,000 iterations, and applied the non-parametric Kruskal-Wallis test followed by the pairwise Wilcoxon test with Holm-Bonferroni

<sup>&#</sup>x27;Supplemental Material. Details on methods, Tables S1 and S2, Figures S1–S4, Appendix S1 (radiocarbon and AAR ages), and Appendix S2 (R script for analyzing the age data). Please visithtps://doi.org/10.1130/GEOL.S.19593418 to access the supplemental material, and contact editing@geosociety.org with any questions.

TABLE 1. SUMMARY STATISTICS FOR THE AGE-FREQUENCY DISTRIBUTIONS OF THE EIGHT TAXA

Taxon	Taxonomic affiliation	N*	Median age (yr B.P.)†	Interquartile age range (yr)	Minimum age (yr B.P.)	Maximum age (yr B.P.)	Age range (yr)	Skewness
Corbula gibba	Bivalvia	25	5695	2229	3318	8917	5599	0.14
Gouldia minima	Bivalvia	30	(5194–6850) 3786 (3362–4868)	(832–3099) 1802 (1128–2633)	2240	7016	4776	0.38
Adelosina intricata	Foraminifera	40	6881	3230	2382	8974	6592	-0.55
Elphidium crispum	Foraminifera	40	(5136–7416) 3194 (0774–4018)	(1907–4502) 2968 (4905–4200)	1126	6785	5659	0.37
Echinocyamus pusillus	Echinoidea	25	(2774–4018) 5472 (4005–5928)	(1865–4360) 1980 (892–3972)	677	7440	6763	-0.88
Psammechinus microtuberculatus- Paracentrotus lividus	Echinoidea	14	4498 (2030–5625)	3640 (2112–5460)	1462	7450	5988	0.09
Pilumnus sp.	Brachyura	17	5709	3011	578	7856	7278	-0.61
Gobius niger	Teleostei	16	(3541–7013) 5198 (3608–6396)	(1528–4785) 2847 (1586–5122)	1396	7637	6241	-0.51

Note: 95% bootstrap confidence intervals for median age and interquartile age range are given in parentheses.

correction to compare median ages of the taxa. Age offset between taxa was calculated as the difference between their median ages.

To evaluate whether taxonomic variation in time averaging is determined by durability, first we tested for correlation between per-taxon IQR and median age. If durability controls time averaging, while the shell input is constant through time and mixing by burrowers is limited to the TAZ, per-taxon IQR and median age should be positively correlated in subsurface increments.

However, sequestration of shells by burrowers or physical mixing below the TAZ and temporal variability in skeletal production can decouple median age and IQR (Tomašových et al., 2014). Second, we assessed whether time averaging is related to mineralogical stability and size of skeletal elements. Finally, we compared the scale of time averaging observed in the shell bed to its extent expected from the net sedimentation rate and the depth of mixing, estimated based on downcore changes in median age of

the increments (see the Supplemental Material). All analyses were performed in R version 4.1.2 (R Core Team, 2021).

#### RESULTS

The median ages of age-frequency distributions (AFDs) differ strongly between the taxa (Kruskal-Wallis test  $\chi^2 = 46.37$ , df = 7, p < 0.001; Table S2) but do not covary with their mineralogy, size, or life habit (Figs. 2 and 3; Table 1; Table S1). Median ages

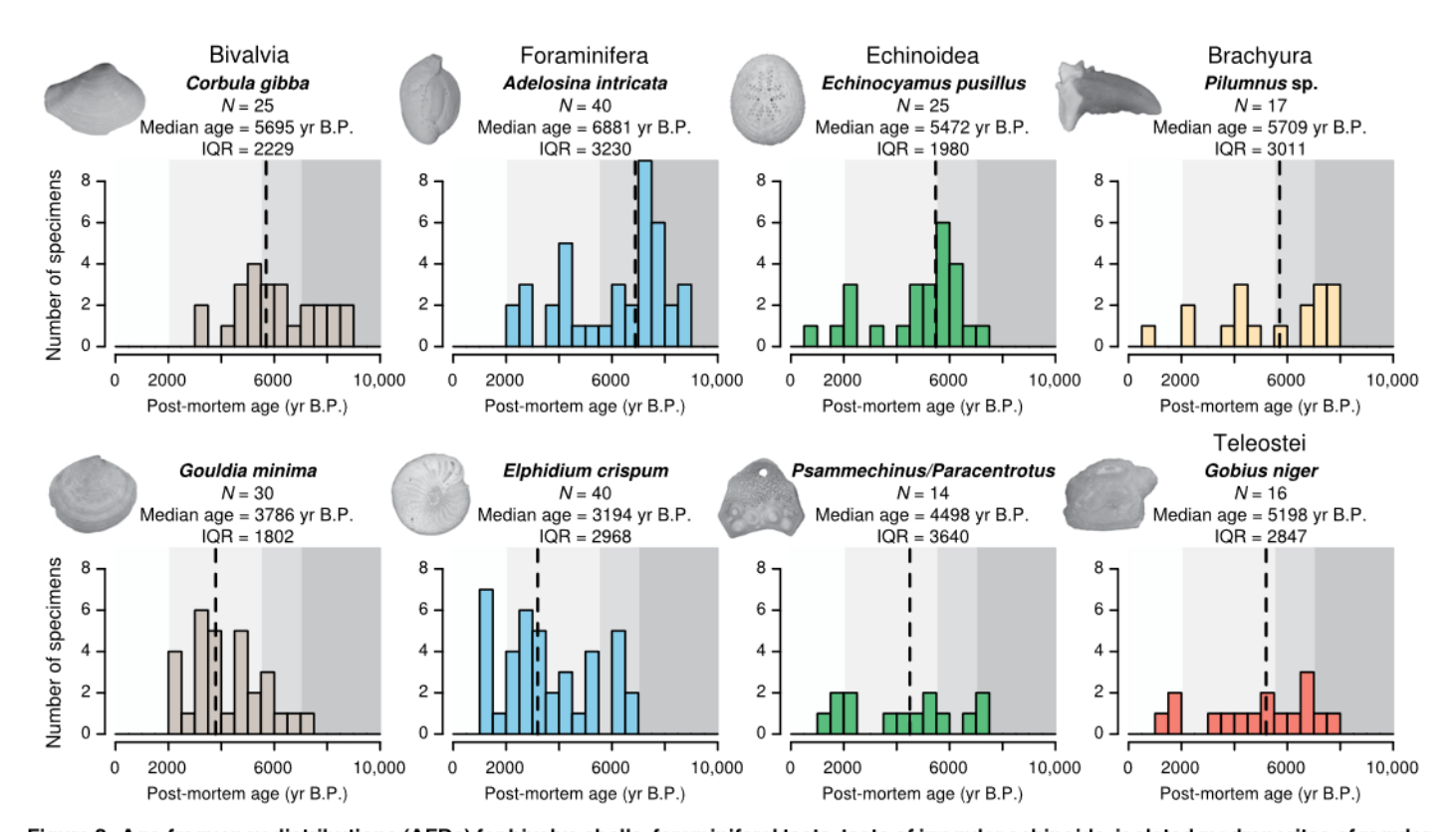


Figure 2. Age-frequency distributions (AFDs) for bivalve shells, foraminiferal tests, tests of irregular echinoids, isolated madreporites of regular echinoids, crab chelae, and fish otoliths in a 10-cm-thick shell bed interval from core Piran 2 M53 (4 km off Piran, Slovenia). AFDs are based on <sup>14</sup>C-calibrated amino acid racemization ages for bivalves and calibrated <sup>14</sup>C ages (median probability ages in 500 yr bins) for all other taxa. Dashed lines represent median ages, and shading marks sea-level phases (see Fig. 1C). IQR—interquartile age range. Photographs are not to scale.

<sup>\*</sup>N-number of dated specimens.

<sup>†</sup>Ages are in years before present (before 1950 CE).

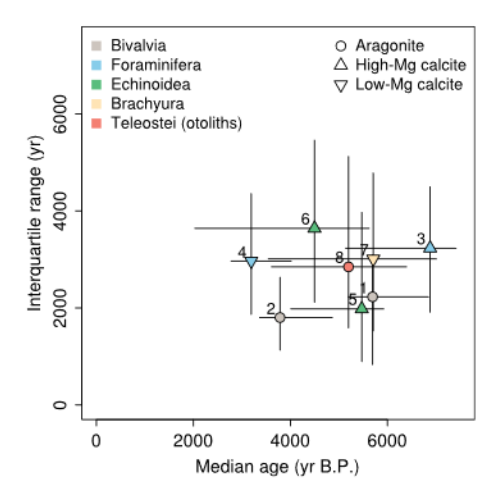


Figure 3. Median ages and interquartile age ranges of eight taxa (interval from core Piran 2 M53, 4 km off Piran, Slovenia) with 95% bootstrap confidence intervals. 1—Corbula gibba; 2—Gouldia minima; 3—Adelosina intricata; 4—Elphidium crispum; 5—Echinocyamus pusillus; 6—Psammechinus microtuberculatus-Paracentrotus lividus; 7—Pilumnus sp.; 8—Gobius niger.

differ by ~3700 yr between the two foraminifera, by ~1900 yr between the two bivalves, and by  $\sim 1000$  yr between the irregular and regular echinoids. The smallest between-species age offset (14 yr) was observed between taxa with fundamentally different skeletal architecture and life habit: the bivalve C. gibba and the crab Pilumnus sp. However, the scale of time averaging is similar across all taxa (Fig. 3; Table 1): IQRs vary from  $\sim$ 1800 yr in G. minima to ~3600 yr in regular echinoids. Median ages and IQRs are not correlated (Pearson r = 0.13, p = 0.75). Neither per-taxon median age nor IOR is related to the average size of the dated elements (Fig. S2), and remains with different mineralogical stability have similar IQRs  $(\sim 3000, 2000-3600, and 1800-2800 \text{ yr for low-}$ Mg calcitic, high-Mg calcitic, and aragonitic taxa, respectively). The extent of time averaging across the taxa is thus independent of their durability. On the other hand, the observed IQRs are very similar to values expected from the net sedimentation rate of 0.006 cm/yr and mixing depth of 10-20 cm estimated for the shell bed interval (expected IQR: 1800-3700 yr; Fig. S3).

# DISCUSSION

# **Absence of Durability Effects**

Our findings demonstrate that remains of taxa with fundamentally different skeletal characteristics, including multi-elemental skeletons of echinoids and crustaceans, can undergo similarly extensive, millennial-scale time averaging. Thus, intrinsic durability, at least among biomineralized taxa, is less important in controlling the duration of time averaging than other factors such as sedimentation rate, sequestration, or temporal variability in production. Similar

scales of time averaging of bivalve, otolith, and foraminiferal assemblages, observed here and in previous studies (Martin et al., 1996; Albano et al., 2020), underscore the lack of significant differences between taxa of different size and skeletal mineralogy. Time averaging of the two foraminifera is nearly identical, even though low-Mg hyaline tests dissolve at lower rates than high-Mg porcelaneous tests in laboratory experiments (Peebles and Lewis, 1991). Thus, just like macrofossils, microfossil records can be time averaged over 10<sup>3</sup> yr in shallow-water sediment-starved environments.

The extensive time averaging of isolated decapod claws and echinoid plates points to their high fossilization potential. These remains can be commonly identified to low taxonomic levels, yet they are commonly overlooked components of death assemblages (Plotnick et al., 1990; Mancosu and Nebelsick, 2020). Decapod cuticles usually undergo rapid decay and fragmentation near the sediment-water interface due to high organic content (Plotnick, 1990). However, claws are the most heavily calcified parts of decapod skeletons (Mutel et al., 2008) and are overrepresented in death assemblages (Stempien, 2005). Similarly, tests of regular echinoids disarticulate rapidly (Kidwell and Baumiller, 1990; Greenstein, 1991), but the large IQR (~3600 yr) of isolated madreporites indicates that individual echinoderm plates can withstand extensive temporal mixing.

The robustness of echinoid plates does not explain, however, the millennial averaging of articulated tests of *E. pusillus* (IQR =  $\sim$ 2000 yr). This value contrasts with yearly time averaging of tests of another clypeasteroid, *Leodia sexiesperforata*, from the Bahamas (IQR = 2 yr; Kowalewski et al., 2018). The two species differ strongly in size, but both have internal support structures and interlocking plates that increase test strength (Grun and Nebelsick, 2018).

# Sequestration and Variability in Skeletal Production

The lack of differences in time averaging between taxa cannot be explained by unusually favorable conditions within the TAZ at Piran: (1) surface sediments in the southern Gulf of Trieste are reworked by storms, well mixed by burrowers (e.g., thalassinidean shrimps; Pervesler and Dworschak, 1985), and undersaturated with respect to aragonite (Ogrinc and Faganeli, 2003); (2) many dated specimens show high taphonomic alteration (Fig. S4); and (3) the shape of the AFD of C. gibba within the fully mixed layer at Piran indicates decadal-scale disintegration rate (Tomašových et al., 2019a). Under slow sedimentation estimated for the shell bed interval, such fast disintegration would lead to time averaging an order of magnitude lower than observed. Our data thus support a sequestration model (Tomašových et al., 2014, 2019b),

in which burial or early diagenetic stabilization in the subsurface buffers against rapid destruction in the TAZ while deep burrowing below the TAZ leads to mixing of skeletal elements of vastly different ages. As skeletal remains are temporally sequestered in the subsurface sediments and occasionally exhumed, this mechanism decouples time averaging from the effect of intrinsic durability. However, initial differences in disintegration rate, prior to sequestration, still lead to over-representation of more robust remains in fossil assemblages.

In spite of similar time averaging, median ages of the eight taxa differ by as much as 10<sup>2</sup>–10<sup>3</sup> yr. These large age offsets most likely resulted from diachronous shifts in local abundance (and thus skeletal production rates) in response to changes in water depth and substrate during the Holocene sea-level rise (Fig. 1C). Upcore replacement of C. gibba by G. minima, preferring muddy and sandy substrates, respectively, produces age offsets between these species persisting throughout the core (Tomašových et al., 2019a). Such age differences between co-occurring taxa are commonly reported from Holocene death assemblages on continental shelves (Kosnik et al., 2009; Krause et al., 2010; Tomašových et al., 2019b).

#### CONCLUSIONS

Our results suggest that sequestration of skeletal remains below the TAZ coupled with slow sedimentation and deep mixing has both positive and negative consequences for paleoecological inferences: taxa differing in durability can have comparable temporal resolution, but significant age offsets between co-occurring species can complicate interspecific analyses of multi-taxic fossil assemblages and make core age models sensitive to taxon choice.

## ACKNOWLEDGMENTS

We are grateful to K. Agiadi for identifying otoliths, M. Kowalewski for discussions, N. Hohmann and S. Macharia for help with sample sorting, and J. Bright for preparing <sup>14</sup>C targets. We thank T. Olszewski and two anonymous reviewers for their comments. This work was supported by the Austrian Science Fund (FWF project P24901) and the Slovak Agency for Research and Development (grant APVV17-0555).

## REFERENCES CITED

Albano, P.G., Hua, Q., Kaufman, D.S., Tomašových, A., Zuschin, M., and Agiadi, K., 2020, Radiocarbon dating supports bivalve-fish age coupling along a bathymetric gradient in high-resolution paleoenvironmental studies: Geology, v. 48, p. 589–593, https://doi.org/10.1130/G47210.1.

Barker, S., Broecker, W., Clark, E., and Hajdas, I., 2007, Radiocarbon age offsets of foraminifera resulting from differential dissolution and fragmentation within the sedimentary bioturbated zone: Paleoceanography, v. 22, PA2205, https:// doi.org/10.1029/2006PA001354.

Bright, J., et al., 2021, Comparing direct carbonate and standard graphite <sup>14</sup>C determinations of biogenic carbonates: Radiocarbon, v. 63, p. 387–403, https://doi.org/10.1017/RDC.2020.131.

- Broecker, W., and Clark, E., 2011, Radiocarbon-age differences among coexisting planktic foraminifera shells: The Barker Effect: Paleoceanography, v. 26, PA2222, https://doi.org/10.1029 /2011PA002116.
- Bush, S.L., Santos, G.M., Xu, X.M., Southon, J.R., Thiagarajan, N., Hines, S.K., and Adkins, J.F., 2013, Simple, rapid, and cost effective: A screening method for <sup>14</sup>C analysis of small carbonate samples: Radiocarbon, v. 55, p. 631–640, https:// doi.org/10.1017/S0033822200057787.
- Gallmetzer, I., Haselmair, A., Tomašových, A., Mautner, A.-K., Schnedl, S.-M., Cassin, D., Zonta, R., and Zuschin, M., 2019, Tracing origin and collapse of Holocene benthic baseline communities in the northern Adriatic Sea: Palaios, v. 34, p. 121–145, https://doi.org/10.2110/palo.2018 068
- Greenstein, B.J., 1991, An integrated study of echinoid taphonomy: Predictions for the fossil record of four echinoid families: Palaios, v. 6, p. 519–540, https://doi.org/10.2307/3514916.
- Grun, T.B., and Nebelsick, J.H., 2018, Structural design of the minute clypeasteroid echinoid *Echinocyamus pusillus*: Royal Society Open Science, v. 5, 171323, https://doi.org/10.1098/ rsos.171323
- Kidwell, S.M., 2013, Time-averaging and fidelity of modern death assemblages: Building a taphonomic foundation for conservation palaeobiology: Palaeontology, v. 56, p. 487–522, https:// doi.org/10.1111/pala.12042.
- Kidwell, S.M., and Baumiller, T., 1990, Experimental disintegration of regular echinoids: Roles of temperature, oxygen, and decay thresholds: Paleobiology, v. 16, p. 247–271, https://doi.org/10.1017/S0094837300009982.
- Kosnik, M.A., Hua, Q., Kaufman, D.S., and Wüst, R.A., 2009, Taphonomic bias and time-averaging in tropical molluscan death assemblages: Differential shell half-lives in Great Barrier Reef sediment: Paleobiology, v. 35, p. 565–586, https://doi .org/10.1666/0094-8373-35.4.565.
- Kowalewski, M., 1997, The reciprocal taphonomic model: Lethaia, v. 30, p. 86–88, https://doi.org /10.1111/j.1502-3931.1997.tb00447.x.
- Kowalewski, M., and Bambach, R.K., 2008, The limits of paleontological resolution, in Harries, P.J., ed., High-Resolution Approaches in Stratigraphic Paleontology: Topics in Geobiology, v. 21, p. 1–48, https://doi.org/10.1007/978-1-4020-9053-0\_1.
- Kowalewski, M., Casebolt, S., Hua, Q., Whitacre,
   K.E., Kaufman, D.S., and Kosnik, M.A., 2018,
   One fossil record, multiple time resolutions:
   Disparate time-averaging of echinoids and mollusks on a Holocene carbonate platform: Geol-

- ogy, v. 46, p. 51–54, https://doi.org/10.1130/ G39789.1.
- Krause, R.A., Jr., Barbour, S.L., Kowalewski, M., Kaufman, D.S., Romanek, C.S., Simões, M.G., and Wehmiller, J.F., 2010, Quantitative comparisons and models of time-averaging in bivalve and brachiopod shell accumulations: Paleobiology, v. 36, p. 428–452, https://doi.org/10.1666/08072.1.
- Lambeck, K., Antonioli, F., Anzidei, M., Ferranti, L., Leoni, G., Scicchitano, G., and Silenzi, S., 2011, Sea level change along the Italian coast during the Holocene and projections for the future: Quaternary International, v. 232, p. 250–257, https:// doi.org/10.1016/j.quaint.2010.04.026.
- Lin, C.H., De Gracia, B., Pierotti, M.E.R., Andrews, A.H., Griswold, K., and O'Dea, A., 2019, Reconstructing reef fish communities using fish otoliths in coral reef sediments: PLoS One, v. 14, e0218413, https://doi.org/10.1371/journal.pone.0218413.
- Mancosu, A., and Nebelsick, J.H., 2020, Tracking biases in the regular echinoid fossil record: The case of *Paracentrotus lividus* in recent and fossil shallow-water, high-energy environments: Palaeontologia Electronica, v. 23, a42, https://doi.org /10.26879/1090.
- Martin, R.E., Wehmiller, J.F., Harris, M.S., and Liddell, W.D., 1996, Comparative taphonomy of bivalves and foraminifera from Holocene tidal flat sediments, Bahia la Choya, Sonora, Mexico (Northern Gulf of California): Taphonomic grades and temporal resolution: Paleobiology, v. 22, p. 80–90, https://doi.org/10.1017/S0094837300016031.
- Mautner, A.-K., Gallmetzer, I., Haselmair, A., Schnedl, S.-M., Tomašových, A., and Zuschin, M., 2018, Holocene ecosystem shifts and human-induced loss of Arca and Ostrea shell beds in the northeastern Adriatic Sea: Marine Pollution Bulletin, v. 126, p. 19–30, https://doi.org/10.1016/j.marpolbul.2017.10.084.
- Mekik, F., 2014, Radiocarbon dating of planktonic foraminifer shells: A cautionary tale: Paleoceanography, v. 29, p. 13–29, https://doi.org/10.1002 /2013PA002532.
- Mutel, M.H.E., Waugh, D.A., Feldmann, R.M., and Parsons-Hubbard, K.M., 2008, Experimental taphonomy of *Callinectes sapidus* and cuticular controls on preservation: Palaios, v. 23, p. 615– 623, https://doi.org/10.2110/palo.2008.p08-024r.
- Ogrinc, N., and Faganeli, J., 2003, Stable carbon isotopes in pore waters of coastal marine sediments (the Gulf of Trieste, N Adriatic): Acta Chimica Slovenica, v. 50, p. 645–662.
- Olszewski, T., 1999, Taking advantage of time-averaging: Paleobiology, v. 25, p. 226–238, https://doi.org/10.1017/S009483730002652X.

- Olszewski, T.D., 2004, Modeling the influence of taphonomic destruction, reworking, and burial on time-averaging in fossil accumulations: Palaios, v. 19, p. 39–50, https://doi.org/10.1669/0883-1351(2004)019<0039:MTIOTD>2
- Peebles, M.W., and Lewis, R.D., 1991, Surface textures of benthic foraminifera from San Salvador, Bahamas: Journal of Foraminiferal Research, v. 21, p. 285–292, https://doi.org/10.2113/gsjfr.21.4.285.
- Pervesler, P., and Dworschak, P.C., 1985, Burrows of *Jaxea nocturna* Nardo in the Gulf of Trieste: Senckenbergiana Maritima, v. 17, p. 33–53.
- Plotnick, R.E., 1990, Paleobiology of the arthropod cuticle: Short Courses in Paleontology, v. 3, p. 177–196, https://doi.org/10.1017/S2475263000001793.
- Plotnick, R.E., McCarroll, S., and Powell, E.N., 1990, Crab death assemblages from Laguna Madre and vicinity, Texas: Palaios, v. 5, p. 81–87, https://doi.org/10.2307/3514998.
- R Core Team, 2021, R: A language and environment for statistical computing, version 4.1.2: Vienna, Austria, R Foundation for Statistical Computing, http://www.r-project.org.
- Stempien, J.A., 2005, Brachyuran taphonomy in a modern tidal-flat environment: Preservation potential and anatomical bias: Palaios, v. 20, p. 400–410, https://doi.org/10.2110/palo.2004.p04-40.
- Tomašových, A., Kidwell, S.M., Barber, R.F., and Kaufman, D.S., 2014, Long-term accumulation of carbonate shells reflects a 100-fold drop in loss rate: Geology, v. 42, p. 819–822, https://doi.org/10.1130/G35694.1.
- Tomašových, A., Gallmetzer, I., Haselmair, A., Kaufman, D.S., Mavrič, B., and Zuschin, M., 2019a, A decline in molluscan carbonate production driven by the loss of vegetated habitats encoded in the Holocene sedimentary record of the Gulf of Trieste: Sedimentology, v. 66, p. 781– 807, https://doi.org/10.1111/sed.12516.
- Tomašových, A., Kidwell, S.M., Alexander, C.R., and Kaufman, D.S., 2019b, Millennial-scale age offsets within fossil assemblages: Result of bioturbation below the taphonomic active zone and out-of-phase production: Paleoceanography and Paleoclimatology, v. 34, p. 954–977, https:// doi.org/10.1029/2018PA003553.
- Trobec, A., et al., 2018, Thickness of marine Holocene sediment in the Gulf of Trieste (northern Adriatic Sea): Earth System Science Data, v. 10, p. 1077–1092, https://doi.org/10.5194/essd-10-1077-2018.

Printed in USA